

Extreme oxygen isotope zoning in garnet and zircon from a metachert block in mélangé reveals metasomatism at the peak of subduction metamorphism

F. Zeb Page¹, Emilia M. Cameron^{1,2}, Clara Margaret Flood¹, Jeffrey W. Dobbins¹, Michael J. Spicuzza², Kouki Kitajima², Ariel Strickland², Takayuki Ushikubo^{2*}, Christopher G. Mattinson³, and John W. Valley²

¹Geology Department, Oberlin College, Oberlin, Ohio 44074, USA

²Wisconsin Secondary Ion Mass Spectrometer Laboratory (WiscSIMS), Department of Geoscience, University of Wisconsin–Madison, Madison, Wisconsin 53706, USA

³Department of Geological Sciences, Central Washington University, Ellensburg, Washington 98926, USA

ABSTRACT

A tectonic block of garnet quartzite in the amphibolite-facies mélangé of the Catalina Schist (Santa Catalina Island, California, USA) records the metasomatic pre-treatment of high- $\delta^{18}\text{O}$ sediments as they enter the subduction zone. The block is primarily quartz, but contains two generations of garnet that record extreme oxygen isotope disequilibrium and inverse fractionations between garnet cores and matrix quartz. Rare millimeter-scale garnet crystals record prograde cation zoning patterns, whereas more abundant ~200- μm -diameter crystals have the same composition as rims on the larger garnets. Garnets of both generations have high- $\delta^{18}\text{O}$ cores (20.8‰–26.3‰, Vienna standard mean ocean water) that require an unusually high- $\delta^{18}\text{O}$ protolith and lower- $\delta^{18}\text{O}$, less variable rims (10.0‰–11.2‰). Matrix quartz values are homogeneous (13.6‰). Zircon crystals contain detrital cores ($\delta^{18}\text{O} = 4.7\text{‰}–8.5\text{‰}$, 124.6 +1.4/–2.9 Ma) with a characteristic igneous trace element composition likely sourced from arc volcanics, surrounded by zircon with metamorphic age (115.1 ± 2.5 Ma) and trace element compositions that suggest growth in the presence of garnet. Metamorphic zircon decreases in $\delta^{18}\text{O}$ from near-core (24.1‰) to rim (12.4‰), in equilibrium with zoned garnets. Collectively, the data document the subduction of a mixed high- $\delta^{18}\text{O}$ siliceous ooze and/or volcanic ash protolith reaching temperatures of 550–625 °C prior to the nucleation of small garnets without influence from external fluids. Metasomatism was recorded in rims of both garnet and zircon populations as large volumes of broadly homogeneous subduction fluids stripped matrix quartz of its extremely high oxygen isotope signature. Thus, zoned garnet and zircon in high- $\delta^{18}\text{O}$ subducted sediments offer a detailed window into subduction fluids.

INTRODUCTION

The nature and timing of mass transfer between the subducting plate and the sub-arc mantle is critical to our understanding of crustal formation at convergent margins and its geochemical signatures. Chemical and mechanical hybridization within subduction mélangé plays an important role in these processes (e.g., Bebout and Penniston-Dorland, 2016), giving rise to models suggesting that partial melting of diapirs of hybridized mélangé rocks is responsible for the classic trace element signature of arc rocks (Marschall and Schumacher, 2012) and

the diversity of magma series found at convergent margins (Cruz-Urbe et al., 2018). Adding to these complications is the recent discovery that some sediments have entered the mantle and melted without mixing or hybridization, preserving extreme oxygen isotope signatures of surface weathering in their neofomed igneous zircon (Spencer et al., 2017). If subducted sediment can regularly carry its characteristically enriched oxygen isotope signature ($\delta^{18}\text{O} = \sim 7\text{‰}–42\text{‰}$, Vienna standard mean ocean water [VSMOW]; Kolodny and Epstein, 1976; Eiler, 2001; Payne et al., 2015) into the mantle ($\delta^{18}\text{O}_{\text{zrc}} = 5.3\text{‰} \pm 0.6\text{‰}$, 2SD [standard deviation]; Valley et al., 1998; Page et al. 2007a), it is surprising that oxygen isotope variability within the sub-arc mantle is so subtle and challenging to measure

(Eiler et al., 1998). A solution to this discrepancy may be found in the fluid metasomatism of subducted sediments.

The first and perhaps most dramatic illustrations of a high degree of fluid flow within subduction mélangé were studies of the oxygen isotope ratios of quartz and carbonate in veins within the Catalina Schist subduction complex (Southern California, USA) suggesting kilometer-scale oxygen isotope homogenization driven by large fluid fluxes (Bebout and Barton, 1989; Bebout, 1991). Over the last quarter century, the Catalina Schist has served as a laboratory for the study of subduction mélangé, with numerous studies detailing fluid metasomatism and mechanical mixing processes in the subduction channel by means of stable isotopes (e.g., Bebout, 1991; Penniston-Dorland et al., 2012), major and trace elements (e.g., Sorensen and Barton, 1987; Hickmott et al., 1992; Penniston-Dorland et al., 2014) and radiogenic isotopes (King et al., 2006).

The *in situ* analysis of oxygen isotopes in garnet is a powerful tool with which to decipher complex or extremely subtle fluid histories and tie them to the metamorphic record. In rocks that have experienced significant metasomatism, the extremely slow intragranular diffusion of oxygen in garnet allows it to preserve a robust geochemical record through all but the hottest and longest of metamorphic events (Vielzeuf et al., 2005). Oxygen isotope variability in garnets from eclogite has illustrated signals of infiltration by mantle (Russell et al., 2013) and supracrustal (e.g., Page et al., 2014; Martin et al., 2014; Rubatto and Angiboust, 2015) fluids that were previously undetectable or not clearly distinguishable using bulk methods.

Chert and siliceous schist are high- $\delta^{18}\text{O}$ lithologies (Eiler, 2001) that are found within the

*Current Address: Kochi Institute for Core Sample Research, JAMSTEC, 200 Monobe-otsu, Nankoku, Kochi 783-8502, Japan

amphibolite-facies Catalina Schist mélangé (Platt, 1975). In this contribution, we explore the metasomatism of a high- $\delta^{18}\text{O}$ garnet- and zircon-bearing metachert from a classic subduction mélangé, in order to better understand the timing and metamorphic conditions of subduction fluid metasomatism, and to gain a more complete picture of how fluids mitigate the influence of high- $\delta^{18}\text{O}$ subduction inputs.

CATALINA GARNET QUARTZITE

Although much less abundant than the better-studied garnet-hornblende lithology, tectonic blocks of garnet quartzite are also found within the amphibolite-facies metasedimentary mélangé of the Catalina Schist (Santa Catalina Island, California), as well as in more coherent, fault-bounded sheets (Platt, 1975; Bebout, 1991). In this study, we report on one exceptional sample of garnet quartzite collected from a meter-scale tectonic block hosted in a shale-matrix mélangé from upper Cottonwood Canyon ($33^{\circ}23'46.20''\text{N}$, $118^{\circ}24'52.80''\text{W}$; Fig. 1A). The quartzite is composed primarily of quartz (93%), garnet (6%), and chlorite (<0.5%), with trace rutile, apatite, amphibole, and zircon (Fig. 1B). Garnet is present in two populations: copious fine-grained (<200- μm -diameter) crystals dispersed throughout the sample, and a smaller number of larger garnets (1–3 mm diameter; Fig. 1B). The larger crystals have abundant inclusions, which are primarily quartz and apatite. X-ray mapping and major element traverses show that the larger garnets display classic prograde cation-zoning profiles with decreasing Mn and increasing Mg# from core to rim, and with rim compositions similar to the compositions of the smaller, more homogeneous (in cations) garnets in the same rock (Figs. 2A and 2B).

Oxygen Isotopes of Quartz and Garnet

Ion microprobe analysis of garnets (Page et al., 2010; see the GSA Data Repository¹ for full data [Tables DR1 and DR2] and methods) shows extreme oxygen isotope zoning; values of $\delta^{18}\text{O}$ are 20.8‰–26.3‰ in garnet cores and 10.0‰–11.2‰ in garnet rims (Fig. 2A). Both large and small garnets in this sample show a similar range in $\delta^{18}\text{O}$, despite the difference in cation zoning and crystal size. Zoning in oxygen isotopes is sharp, with as much as a 7‰ drop in $\delta^{18}\text{O}$ over a few micrometers, whereas cation zoning is much more gradual, with slightly increased Ca and Mg in the rims of larger garnets (Fig. 2). Smaller garnets are nearly homo-

¹GSA Data Repository item 2019232, methods; equilibrium assemblage diagram; $\delta^{18}\text{O}$ analyses of garnet, zircon, and quartz standards and unknowns by SIMS; U-Pb isotope and trace element analyses of zircon by SHRIMP; cathodoluminescence images of zircon with analysis spot locations; and back-scattered electron images of garnet and quartz with analysis locations, is available online at <http://www.geosociety.org/datarepository/2019/>, or on request from editing@geosociety.org.

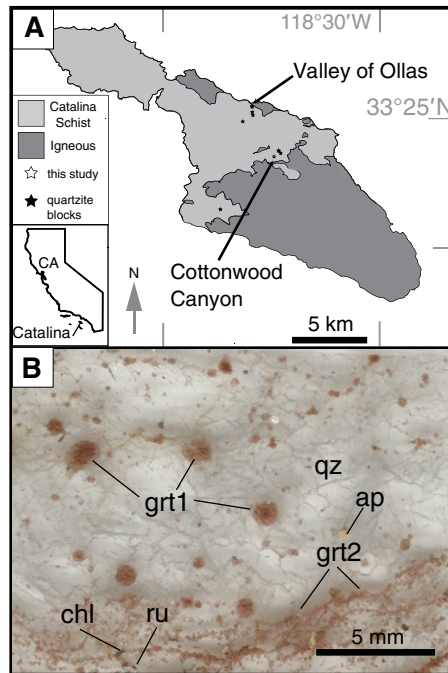


Figure 1. A: Geologic sketch map of Santa Catalina Island, California (CA), USA (after Platt, 1975), showing sample locations. **B:** Polished thick section of garnet quartzite showing two garnet sizes (grt1—larger, cation-zoned garnet; grt2—smaller garnet crystals, homogeneous in cations). qz—quartz; ru—rutile; ap—apatite; chl—chlorite.

geneous, with a slight increase in Mg# from core to rim. Matrix quartz has no systematic zoning in cathodoluminescence (CL) imaging and is homogeneous in $\delta^{18}\text{O}$, with ion microprobe analyses (13.5‰) identical (within uncertainty) to bulk (~2 mg) analysis by laser fluorination (13.6‰). Garnet-core and quartz pairs yield reversed fractionations ($\delta^{18}\text{O}_{\text{grt1}} > \delta^{18}\text{O}_{\text{qz}}$), indicat-

ing profound disequilibrium. Eleven analyses of quartz inclusions in large garnet cores yield $\delta^{18}\text{O} = 13.8\text{‰}–16.2\text{‰}$, higher than in matrix quartz, but not in equilibrium with host garnet. Inclusions were generally >50 μm , and commonly along cracks and so are unlikely to preserve their original values.

Oxygen Isotopes in Zircon

Zircons were separated from the sample and mounted in epoxy for analysis (see the Data Repository). CL imaging (Fig. 3A) reveals oscillatory-zoned cores, commonly as fragments of crystals, containing inclusions of quartz, K-feldspar, and biotite. These detrital cores are surrounded by annuli of variable-CL-intensity, somewhat mottled zircon, containing inclusions of quartz, biotite, sphene, and rutile. Outside of this mottled zone, zircons typically have darker-CL-intensity oscillatory-zoned rims, with rare crystals containing a brighter outer rim with faint oscillatory zoning.

Zircons were analyzed for their oxygen isotope ratios by ion microprobe using both a ~15- μm - and a sub-1- μm -diameter beam (Tables DR4, DR5). Highly precise and accurate oxygen isotope ratios from the larger analysis pits are correlated with CL zonation and inclusion population. Zircon cores ($n = 7$) have $\delta^{18}\text{O}$ from 4.7‰ to 8.4‰ (Figs. 3A and 3B). Zircon with mottled CL immediately outside of detrital cores ($n = 17$) has an extremely high $\delta^{18}\text{O}$ of $22.6\text{‰} \pm 3.3\text{‰}$ (2 SD, of 17 analyses in this zone) if one anomalously low analysis is discounted. Intermediate-CL-intensity oscillatory-zoned rims ($n = 20$) have lower $\delta^{18}\text{O}$ values ($17.3\text{‰} \pm 3.9\text{‰}$), and rare bright outer rims have lower-still $\delta^{18}\text{O}$ values ($12.9\text{‰} \pm 3.3\text{‰}$).

To further determine if there is a systematic zoning pattern in zircon like that found in garnet,

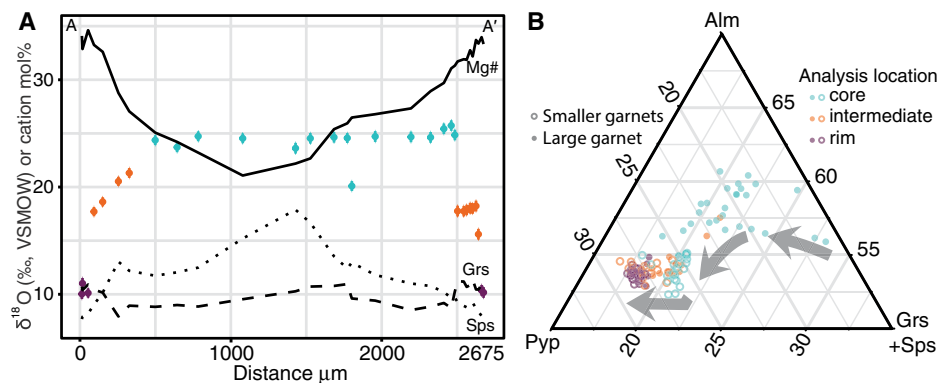


Figure 2. A: $\delta^{18}\text{O}$ and cation traverse, rim to rim, of single ~2.5-mm-diameter garnet. Core region is generally homogeneous in $\delta^{18}\text{O}$ at ~25‰ (aquamarine symbols) and transitions to intermediate values (orange) and low- $\delta^{18}\text{O}$, ~10‰ rims (purple) over short intervals, although zoning is asymmetric. Mg# (Mg / [Mg + Fe], solid line) increases continuously core to rim. VSMOW—Vienna standard mean ocean water. **B:** Ternary diagram of garnet cation compositions; millimeter-scale garnets are shown as solid circles, ~100- μm -scale garnets as open circles. Analysis location (core, intermediate, rim) is also correlated with $\delta^{18}\text{O}$, and indicated by color, as in A. Larger garnets have greater cation zoning than smaller garnets (dashed arrow), and all oxygen isotope zonation takes place at the most pyrope-rich compositions for both sizes. Gray arrow shows core to rim cation zoning of larger garnets. Alm—almandine; Pyp—pyrope; Grs—grossular; Sps—spessartine.

Figure 3. Catalina Schist (Santa Catalina Island, California, USA) quartzite zircon chemistry and age. A: Cathodoluminescence (CL) images (25 μm scale bars) of three zircons showing different CL domains (see text for details) and three types of *in situ* analyses. U-Pb isotope analyses are labelled with $^{238}\text{U}/^{206}\text{Pb}$ age \pm 2SD [standard deviations]. Larger $\delta^{18}\text{O}$ analyses (\sim 15 μm spots, \pm 0.2–0.4‰ 2SD) are labeled with values in per mil, relative to Vienna standard mean ocean water (VSMOW). Sub-micrometer spot analyses (\pm 2.5‰ 2SD) appear as arrays of small dots and are labelled with averages of each CL zone (\pm 2SD) in per mil relative to VSMOW. B: Histogram of all $\delta^{18}\text{O}$ analyses of zircon and garnet with a 15- μm -diameter spot size grouped by CL domain (bright, dark, mottled) for zircon, and location across multiple traverses for garnet; colors as in Figure 2.

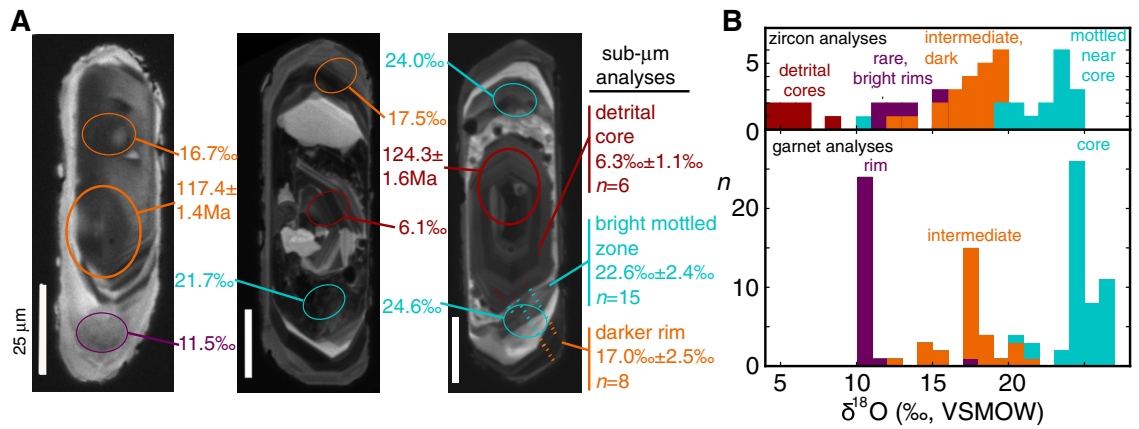


Figure 3. Catalina Schist (Santa Catalina Island, California, USA) quartzite zircon chemistry and age. A: Cathodoluminescence (CL) images (25 μm scale bars) of three zircons showing different CL domains (see text for details) and three types of *in situ* analyses. U-Pb isotope analyses are labelled with $^{238}\text{U}/^{206}\text{Pb}$ age \pm 2SD [standard deviations]. Larger $\delta^{18}\text{O}$ analyses (\sim 15 μm spots, \pm 0.2–0.4‰ 2SD) are labeled with values in per mil, relative to Vienna standard mean ocean water (VSMOW). Sub-micrometer spot analyses (\pm 2.5‰ 2SD) appear as arrays of small dots and are labelled with averages of each CL zone (\pm 2SD) in per mil relative to VSMOW. B: Histogram of all $\delta^{18}\text{O}$ analyses of zircon and garnet with a 15- μm -diameter spot size grouped by CL domain (bright, dark, mottled) for zircon, and location across multiple traverses for garnet; colors as in Figure 2.

29 sub-1 μm analyses (following the method of Page et al. [2007b]) were made in traverses across a single zircon (Fig. 3A). These high-spatial-resolution (but less precise, \pm 0.9‰–1.7‰, 2 SD) analyses confirm the presence of a low- $\delta^{18}\text{O}$ core (6.3‰ \pm 1.1‰, 2 SD, n = 6), surrounded by an extremely high- $\delta^{18}\text{O}$ mottled-CL region (22.6‰ \pm 2.4‰, n = 15), indistinguishable within the uncertainty of the sub-1 μm data from the 15- μm -diameter analyses of the same zones. An outer, darker oscillatory-zoned rim has $\delta^{18}\text{O}$ of 17.0‰ \pm 2.5‰ (n = 8). The zircon chosen for this analysis does not have an outermost, lighter rim.

PRESSURE, TEMPERATURE, AND TIME HISTORY

The limited mineralogy of this sample, coupled with its metasomatic history and zoned minerals, makes thermobarometry challenging. However, an equilibrium assemblage diagram calculated using an estimate of the bulk composition and the computer package *Perple_X* (Connolly, 2009; <http://www.perplex.ethz.ch>; Fig. DR1) yields reasonable results. The observed assemblage (quartz + garnet + rutile \pm chlorite) is expected to form at pressures >0.8 GPa and temperatures >550 $^{\circ}\text{C}$. The core-to-rim increase of Mg# observed in the large garnets is consistent with growth during increasing temperatures in the presence of chlorite, and is calculated by the model to have taken place at \sim 550–650 $^{\circ}\text{C}$ at pressures of >1.1 GPa, consistent with existing pressure and temperature estimates of amphibolite blocks in the same mélangé and [Zr]-in-rutile thermometry from this same sample (Sorensen and Barton, 1987; Hartley et al., 2016; Penniston-Dorland et al., 2018). The closeness between the conditions calculated by the model and existing thermobarometry from the Catalina Schist suggests that the metasomatism of this block did not involve substantial change in cation composition. Regardless of the precise conditions of metamorphism, the concomitant decrease in $\delta^{18}\text{O}$ with

increasing Mg# in garnet requires metasomatism as the sample increased in temperature within the subduction environment.

Zircons were additionally analyzed by sensitive high-resolution ion microprobe–reverse geometry (SHRIMP-RG) for U-Pb isotopes and select trace elements (see the Data Repository). Detrital zircon cores have more elevated Th/U ratios (0.36–0.89) and are older than rims; eight of nine analyses yield a coherent ^{204}Pb -corrected $^{206}\text{Pb}^*/^{238}\text{U}$ age of 124.6 \pm 1.4/–2.9 Ma (Fig. DR6). Th/U ratios of rims are lower (0.02–0.13) and yield an age of 115.1 \pm 2.4 Ma, consistent with an igneous origin for zircon cores and a metamorphic one for the rims (Fig. DR6). Zircon rims also have smaller Eu anomalies (Eu/Eu* \sim 1) and flatter heavy rare earth element patterns, consistent with a metamorphic origin in a garnet-present, plagioclase-absent high-pressure environment (Fig. DR6).

DISCUSSION

Taken together, the pressure-temperature-time-fluid data preserved in garnet and zircon from this sample provide a detailed record of metasomatic events within the subduction channel. A mixed-lithology protolith containing both extremely high- $\delta^{18}\text{O}$ siliceous material intermixed with intermediate and/or mafic igneous material including detrital igneous zircon grains was subducted between 124 and 115 Ma. The most plausible interpretation is that the protolith was a mixture of chert or siliceous ooze mixed with ca. 124 Ma arc volcanoclastic material. The relative purity of the quartzite and the narrow range of zircon core ages seem to preclude weathering of plutonic source material as an origin for the inherited cores. This mixed sediment was subducted and metamorphosed initially as a closed system, with larger, prograde garnet cores having high and unchanging $\delta^{18}\text{O}$ values. The extreme oxygen isotope ratio of this sample ($\delta^{18}\text{O}$ values in quartz in equilibrium with garnet cores at 550 $^{\circ}\text{C}$ would have been >30‰; Valley, 2003) makes it highly sensitive

to infiltration from external fluids with lower $\delta^{18}\text{O}$. A second generation of garnets nucleated near the peak of metamorphism, but their growth was not initiated by an external fluid, as core $\delta^{18}\text{O}$ compositions are identical to those of larger garnets. As metamorphic temperatures reached their peak, an external fluid permeated the sample, perhaps due to introduction of the block into the subduction mélangé, shifting matrix quartz $\delta^{18}\text{O}$ from \sim 30‰ to 13.6‰. Slow rates of intragranular diffusion preserve a record of the original high- $\delta^{18}\text{O}$ composition of garnet and zircon, and their continued growth documents decreasing $\delta^{18}\text{O}$ from \sim 24‰ to \sim 17‰ to \sim 11‰, possibly in two discrete pulses. Fractionation between matrix quartz and garnet rim compositions yields temperatures of \sim 600–750 $^{\circ}\text{C}$ (Valley, 2003), consistent with estimates of peak metamorphic temperatures for the block and the region. Likewise, garnet cation composition records increasing temperature (pressure is not well constrained) during metasomatism. Perhaps upwelling within the subduction channel stopped quartz recrystallization and garnet growth simultaneously, effectively ending the record preserved in this sample.

The limited range of $\delta^{18}\text{O}$ in quartz and calcite veins within the Catalina Schist first reported by Bebout and Barton (1989) suggests that the entire package of subduction rocks on Catalina Island interacted with a remarkably homogeneous supracrustal fluid reservoir derived from metamorphic dehydration of minerals deeper along the subducting slab with an oxygen isotope composition of 13‰ \pm 1.0‰. The quartz $\delta^{18}\text{O}$ value for the block in mélangé in this study (13.6‰) yields a calculated water $\delta^{18}\text{O}$ value of 12.3‰ (650 $^{\circ}\text{C}$; Friedman and O’Neil, 1977), in close agreement with the range reported by Bebout and Barton (1989).

Although high- $\delta^{18}\text{O}$ sediments make up a volumetrically small portion of subducted material, the extreme contrast between their isotope ratios and those of the mantle make them likely candidates for introducing fine-scale iso-

tope anomalies in the sub-arc mantle. Indeed, the recent discovery of extremely high- $\delta^{18}\text{O}$ zircons in S-type granites within the supra-subduction-zone mantle of the Oman-UAE ophiolite (Spencer et al., 2017) as well as this contribution show that this can happen. The sample documented in this study is an example of the most extreme contrast in $\delta^{18}\text{O}$ that one might expect to be subducted, with an estimated protolith $\delta^{18}\text{O}$ of 30‰. However, the metasomatic processes documented by garnet and zircon zonation in this metachert from the Catalina Schist show that subduction fluids can all but wipe out extremely high- $\delta^{18}\text{O}$ inputs to subduction zones. Given the modest modal proportion of garnet (7%) with respect to quartz (93%) in this sample, and assuming $\delta^{18}\text{O}$ values of 24‰ for garnet and 14‰ for quartz, the whole-rock $\delta^{18}\text{O}$ of this rock must be <15‰, a value that can also be found in the much more abundant subducted metabasalts with protoliths enriched in ^{18}O by low-temperature interaction with seawater (Eiler, 2001). Subduction fluids play a vital role in the generation of arc magmatism and continental growth, but it also seems that they play an important role in buffering the $\delta^{18}\text{O}$ of rocks that are recycled into the mantle by subduction, with only strongly refractory (and volumetrically minor) phases such as zircon and garnet able to carry extreme oxygen isotope ratios into the mantle.

ACKNOWLEDGMENTS

We thank Eric Essene, who provided mentorship, assistance in the field, and partial funding for secondary ion mass spectrometry (SIMS) analysis; S. Penniston-Dorland, E. Walsh, and the 2012 Keck Catalina Project (National Science Foundation [NSF] REU-1062720) students for assistance with fieldwork on Catalina Island; and the Catalina Island Conservancy for access and field support. Comments from Christopher Spencer, two anonymous reviewers, and editor Chris Clarke improved this manuscript. Assistance with SHRIMP analyses was provided by J. Wooden and F. Mazdab (U.S. Geological Survey), and assistance with electron microprobe analyses by G. Moore (University of Michigan, USA) are gratefully acknowledged. The WiscSIMS ion microprobe laboratory is supported by the National Science Foundation (grants EAR-1355590, EAR-1658823) and the University of Wisconsin–Madison. Page, Cameron, Flood, and Dobbins gratefully acknowledge financial support from Oberlin College (Ohio, USA) and the NSF (grant EAR-1249778). Valley is supported by the NSF (grant EAR-1524336).

REFERENCES CITED

Bebout, G.E., 1991, Field-based evidence for devolatilization in subduction zones: Implications for arc magmatism: *Science*, v. 251, p. 413–416, <https://doi.org/10.1126/science.251.4992.413>.
 Bebout, G.E., and Barton, M.D., 1989, Fluid flow and metasomatism in a subduction zone hydrothermal system: Catalina Schist terrane, California: *Geology*, v. 17, p. 976–980, [https://doi.org/10.1130/0091-7613\(1989\)017<0976:FFAMIA>2.3.CO;2](https://doi.org/10.1130/0091-7613(1989)017<0976:FFAMIA>2.3.CO;2).
 Bebout, G.E., and Penniston-Dorland, S.C., 2016, Fluid and mass transfer at subduction interfaces—The field metamorphic record: *Lithos*, v. 240–243, p. 228–258, <https://doi.org/10.1016/j.lithos.2015.10.007>.
 Connolly, J.A.D., 2009, The geodynamic equation of state: What and how: *Geochemistry Geophysics*

Geosystems, v. 10, Q10014, <https://doi.org/10.1029/2009GC002540>.
 Cruz-Urbe, A.M., Marschall, H.R., Gaetani, G.A., and Le Roux, V., 2018, Generation of alkaline magmas in subduction zones by partial melting of mélange diapirs—An experimental study: *Geology*, v. 46, p. 343–346, <https://doi.org/10.1130/G39956.1>.
 Eiler, J.M., 2001, Oxygen isotope variations of basaltic lavas and upper mantle rocks, in Valley, J.W. and Cole, D.R. eds., *Stable Isotope Geochemistry: Reviews in Mineralogy and Geochemistry*, v. 43, p. 319–364, <https://doi.org/10.1515/9781501508745-008>.
 Eiler, J.M., McInnes, B., Valley, J.W., Graham, C.M., and Stolper, E.M., 1998, Oxygen isotope evidence for slab-derived fluids in the sub-arc mantle: *Nature*, v. 393, p. 777–781, <https://doi.org/10.1038/31679>.
 Friedman, I., and O'Neil, J.R., 1977, Compilation of stable isotope fractionation factors of geochemical interest: U.S. Geological Survey Professional Paper 440-KK, 11 p., <https://doi.org/10.3133/pp440KK>.
 Hartley, E.S., Pereira, I., Moreira, H., Page, F.Z., and Storey, C.D., 2016, Petrology and trace element thermometry of garnet-quartzite from the Catalina Schist: *Geological Society of America Abstracts with Programs*, v. 48, no. 7, <https://doi.org/10.1130/abs/2016AM-282181>.
 Hickmott, D.D., Sorensen, S.S., and Rogers, P.S.Z., 1992, Metasomatism in a subduction complex: Constraints from microanalysis of trace elements in minerals from garnet amphibolite from the Catalina Schist: *Geology*, v. 20, p. 347–350, [https://doi.org/10.1130/0091-7613\(1992\)020<0347:MIASCC>2.3.CO;2](https://doi.org/10.1130/0091-7613(1992)020<0347:MIASCC>2.3.CO;2).
 King, R.L., Bebout, G.E., Moriguti, T., and Nakamura, E., 2006, Elemental mixing systematics and Sr-Nd isotope geochemistry of mélange formation: Obstacles to identification of fluid sources to arc volcanics: *Earth and Planetary Science Letters*, v. 246, p. 288–304, <https://doi.org/10.1016/j.epsl.2006.03.053>.
 Kolodny, Y., and Epstein, S., 1976, Stable isotope geochemistry of deep sea cherts: *Geochimica et Cosmochimica Acta*, v. 40, p. 1195–1209, [https://doi.org/10.1016/0016-7037\(76\)90155-1](https://doi.org/10.1016/0016-7037(76)90155-1).
 Marschall, H.R., and Schumacher, J.C., 2012, Arc magmas sourced from mélange diapirs in subduction zones: *Nature Geoscience*, v. 5, p. 862–867, <https://doi.org/10.1038/ngeo1634>.
 Martin, L.A., Rubatto, D., Crépisson, C., Hermann, J., Putlitz, B., and Vitale-Browarone, A., 2014, Garnet oxygen analysis by SHRIMP-SI: Matrix corrections and application to high-pressure metamorphic rocks from Alpine Corsica: *Chemical Geology*, v. 374–375, p. 25–36, <https://doi.org/10.1016/j.chemgeo.2014.02.010>.
 Page, F.Z., Fu, B., Kita, N.T., Fournelle, J., Spicuzza, M.J., Schulze, D.J., Viljoen, F., Basei, M., and Valley, J.W., 2007a, Zircon from kimberlite: New insights from oxygen isotopes, trace elements, and Ti in zircon thermometry: *Geochimica et Cosmochimica Acta*, v. 71, p. 3887–3903, <https://doi.org/10.1016/j.gca.2007.04.031>.
 Page, F.Z., Ushikubo, T., Kita, N.T., Riciputi, L.R., and Valley, J.W., 2007b, High-precision oxygen isotope analysis of picogram samples reveals 2 μm gradients and slow diffusion in zircon: *The American Mineralogist*, v. 92, p. 1772–1775, <https://doi.org/10.2138/am.2007.2697>.
 Page, F.Z., Kita, N.T., and Valley, J.W., 2010, Ion microprobe analysis of oxygen isotopes in garnets of complex chemistry: *Chemical Geology*, v. 270, p. 9–19, <https://doi.org/10.1016/j.chemgeo.2009.11.001>.
 Page, F.Z., Essene, E.J., Mukasa, S.B., and Valley, J.W., 2014, A garnet-zircon oxygen isotope

record of subduction and exhumation fluids from the Franciscan Complex, California: *Journal of Petrology*, v. 55, p. 103–131, <https://doi.org/10.1093/petrology/egt062>.
 Payne, J.L., Hand, M., Pearson, N.J., Barovich, K.M., and McInerney, D.J., 2015, Crustal thickening and clay: Controls on O isotope variation in global magmatism and siliciclastic sedimentary rocks: *Earth and Planetary Science Letters*, v. 412, p. 70–76, <https://doi.org/10.1016/j.epsl.2014.12.037>.
 Penniston-Dorland, S.C., Bebout, G.E., Pogge von Strandmann, P.A.E., Elliott, T., and Sorensen, S.S., 2012, Lithium and its isotopes as tracers of subduction fluids and metasomatic processes: Evidence from the Catalina Schist, California, USA: *Geochimica et Cosmochimica Acta*, v. 77, p. 530–545, <https://doi.org/10.1016/j.gca.2011.10.038>.
 Penniston-Dorland, S.C., Gorman, J.K., Bebout, G.E., Piccoli, P.M., and Walker, R.J., 2014, Reaction rind formation in the Catalina Schist: Deciphering a history of mechanical mixing and metasomatic alteration: *Chemical Geology*, v. 384, p. 47–61, <https://doi.org/10.1016/j.chemgeo.2014.06.024>.
 Penniston-Dorland, S.C., Kohn, M.J., and Piccoli, P.M., 2018, A mélange of subduction temperatures: Evidence from Zr-in-rutile thermometry for strengthening of the subduction interface: *Earth and Planetary Science Letters*, v. 482, p. 525–535, <https://doi.org/10.1016/j.epsl.2017.11.005>.
 Platt, J.P., 1975, Metamorphic and deformational processes in the Franciscan Complex, California: Some insights from the Catalina Schist terrane: *Geological Society of America Bulletin*, v. 86, p. 1337–1347, [https://doi.org/10.1130/0016-7606\(1975\)86<1337:MADPIT>2.0.CO;2](https://doi.org/10.1130/0016-7606(1975)86<1337:MADPIT>2.0.CO;2).
 Rubatto, D., and Angiboust, S., 2015, Oxygen isotope record of oceanic and high-pressure metamorphism: A P-T-time-fluid path for the Monviso eclogites (Italy): *Contributions to Mineralogy and Petrology*, v. 170, p. 1–16, <https://doi.org/10.1007/s00410-015-1198-4>.
 Russell, A.K., Kitajima, K., Strickland, A., Medaris, L.G., Jr., Schulze, D.J., and Valley, J.W., 2013, Eclogite-facies fluid infiltration: Constraints from $\delta^{18}\text{O}$ zoning in garnet: *Contributions to Mineralogy and Petrology*, v. 165, p. 103–116, <https://doi.org/10.1007/s00410-012-0794-9>.
 Sorensen, S.S., and Barton, M., 1987, Metasomatism and partial melting in a subduction complex—Catalina Schist, Southern California: *Geology*, v. 15, p. 115–118, [https://doi.org/10.1130/0091-7613\(1987\)15<115:MAPMIA>2.0.CO;2](https://doi.org/10.1130/0091-7613(1987)15<115:MAPMIA>2.0.CO;2).
 Spencer, C.J., Cavois, A.J., Raub, T.D., Rollinson, H., Jeon, H., Searle, M.P., Miller, J.A., McDonald, B.J., Evans, N.J., and the Edinburgh Ion Microprobe Facility (EIMF), 2017, Evidence for melting mud in Earth's mantle from extreme oxygen isotope signatures in zircon: *Geology*, v. 45, p. 975–978, <https://doi.org/10.1130/G39402.1>.
 Valley, J.W., 2003, Oxygen isotopes in zircon: Reviews in Mineralogy and Geochemistry, v. 53, p. 343–385, <https://doi.org/10.2113/0530343>.
 Valley, J.W., Kinny, P., Schulze, D.J., and Spicuzza, M.J., 1998, Zircon megacrysts from kimberlite: Oxygen isotope variability among mantle melts: *Contributions to Mineralogy and Petrology*, v. 133, p. 1–11.
 Vielzeuf, D., Veschambre, M., and Brunet, F., 2005, Oxygen isotope heterogeneities and diffusion profile in composite metamorphic-magmatic garnets from the Pyrenees: *The American Mineralogist*, v. 90, p. 463–472, <https://doi.org/10.2138/am.2005.1576>.

Printed in USA